Title:

Secular change and inter-annual variability of the Gulf Stream position, 1993-2013, 70°-55° W

Authors:

James J. Bisagni[1] and Avijit Gangopadhyay
University of Massachusetts, Dartmouth
School for Marine Science and Technology
200 Mill Rd., Suite 325
Fairhaven, MA, USA
02719

Alejandra Sanchez-Franks
National Oceanography Centre
Southampton, UK
SO14 3ZH

[1]Corresponding Author: jbisagni@umassd.edu, (508) 910-6328

Abstract:

The Gulf Stream (GS) is the northeastward-flowing surface limb of the Atlantic Ocean's meridional overturning circulation (AMOC) "conveyer belt" that flows towards Europe and the Nordic Seas. Changes in the GS position after its separation from the coast at Cape Hatteras, i.e., from 75°W to 50°W, may be key to understanding the AMOC, sea level variability and ecosystem behavior along the east coast of North America. In this study we compare secular change and inter-annual variability (IAV) of the Gulf Stream North Wall (GSNW) position with equator-ward Labrador Current (LC) transport along the southwestern Grand Banks near 52° W using 21 years (1993-2013) of satellite altimeter data. Results at 55°, 60°, and 65° W show a significant southward (negative) secular trend for the GSNW, decreasing to a small but insignificant southward trend at 70° W. IAV of de-trended GSNW position residuals also decreases to the west. The long-term secular trend of annual mean upper layer (200 m) LC transport near 52° W is positive. Furthermore, IAV of LC transport residuals near 52° W along the southwestern Grand Banks are significantly correlated with GSNW position residuals at 55° W at a lag of +1-year, with positive (negative) LC transport residuals corresponding to southward (northward) GSNW positions one year later. The Taylor-Stephens index (TSI) computed from the first principal component of the GSNW position from 79° to 65° W shows a similar relationship with a more distal LC index computed along altimeter ground track 250 located north of the Grand Banks across Hamilton Bank in the western Labrador Sea. Increased (decreased) sea height differences along ground track 250 are significantly correlated with a more southward (northward) TSI two years later (lag of +2-years). Spectral analysis of IAV reveals corresponding spectral peaks at 5-7 years and 2-3 years for the North Atlantic Oscillation (NAO), GSNW (70°-55°W) and LC transport near 52° W for the 1993-2013 period suggesting a connection between these phenomena. An upper-layer (200 m) slope water volume calculation using the LC IAV rms residual of +1.04 Sv near 52° W results in an estimated GSNW IAV residual of 79 km, or 63% of the observed 125.6 km (1.13°) rms value at 55° W. A similar upper-layer slope water volume calculation using the positive long-term, upper-layer LC transport trend accounts for 68% of the mean observed secular southward shift of the GSNW between 55° and 70°W over the 1993-2013 period. Our work provides additional observational evidence of important interactions between the upper layers of the sub-polar and sub-tropical gyres within the North Atlantic over both secular and inter-annual time scales as suggested by previous studies.

Introduction:

The Gulf Stream (GS) and Labrador Current (LC) form the western boundary currents of the sub-tropical and sub-polar gyres of the North Atlantic, respectively, meeting near the Tail of the Grand Banks (TGB). At the TGB, a large fraction of the LC turns eastward and joins the GS to form the North Atlantic Current (NAC) that continues flowing towards Europe and the Nordic Seas. The remaining LC fraction flows equator-ward around the TGB along the seaward edge of the Canadian and U.S. continental shelves. An examination of geostrophic surface velocity vectors (Fig. 1) (calculated from 1993-2013, Ssalto/Duacs altimetry products, *in situ* data, MSS_CNES-CLS11 Mean Sea Surface, and the EGM-DIR-R4 geoid model, combining data from both GOCE and GRACE geoid models), clearly shows this general large-scale circulation in the western North Atlantic: the northeastward-flowing GS from Cape Hatteras to south of the TGB, its mean location observed in the large velocities located between the anti-cyclonic sub-tropical gyre and the Northern Recirculation Gyre (NRG). Moving north, at the TGB, the GS evolves into the meandering NAC, distending in and out of the Northwest Corner. Patterns of low dynamic height within the Labrador Basin are characteristic of the cyclonic sub-polar gyre with the LC flowing southeast and equatorward around the Grand Banks. The strongest LC signal is located along the 500 m isobath from the north just off Labrador near altimeter ground track 250, southward to the west of the Flemish Cap, and then around the Grand Banks (Fig. 1). Sinking of cold dense water in the Labrador Sea flows southward along the outer continental slope and rise (not shown) to form the Deep Western Boundary Current (DWBC), forming the southward-flowing subsurface limb of the Atlantic Ocean's meridional overturning circulation (AMOC), with the GS forming the AMOC's northward-flowing surface limb. Inputs from the Greenland, Iceland, and Norwegian Sea (not shown) also form an important southward-flowing sub-surface portion of the AMOC described in summary by Yashayaev *et al*. (2015).

The space-time variability of the latitudinal excursion of the GS "north wall" (GSNW) has been shown by combined observational and modeling studies to be an important diagnostic variable and indicator of the AMOC's amplitude (Joyce and Zhang, 2010; Sanchez-Franks and Zhang, 2015). A stronger (weaker) AMOC corresponded to a more southerly (northerly) GSNW using a GFDL climate model and satellite-derived data, respectively (Joyce and Zhang, 2010). Cooler temperatures, lower salinities, and low planetary potential vorticity characteristic of Labrador Sea Water (LSW), along with stronger southwestward flow, were in phase within Slope Waters located between the shelf break and the GSNW from 1993-2007, and preceded a southward shift of the GSNW by 6 months (Peña-Molino and Joyce, 2008) in agreement with Rossby (1999), Rossby and Benway (2000), and Flagg *et al*. (2006). Direct observations of the DWBC along the "Line-W" array located northwest of Bermuda show similar results with stronger DWBC transport when the GSNW is displaced to the south (Toole *et al*., 2011). More recent studies have shown that in addition to seasonal and short timescale variability, strong inter-annual variability (IAV) of the AMOC has also occurred, with a 30% reduction in AMOC transport between 1 April 2009 and 31 March 2010 along the RAPID/WATCH 26°N measurement array (McCarthy *et al*., 2012; Smeed *et al*., 2014). This reduction in the AMOC was accompanied by a stronger Slope Water current, but does not support the Slope Current as a significant driver of GS position by itself, which may also partly result from the supply of source waters from the Labrador Sea and the sub-polar gyre (Rossby, 1999; Ezer and Atkinson, 2014; Ezer, 2015).

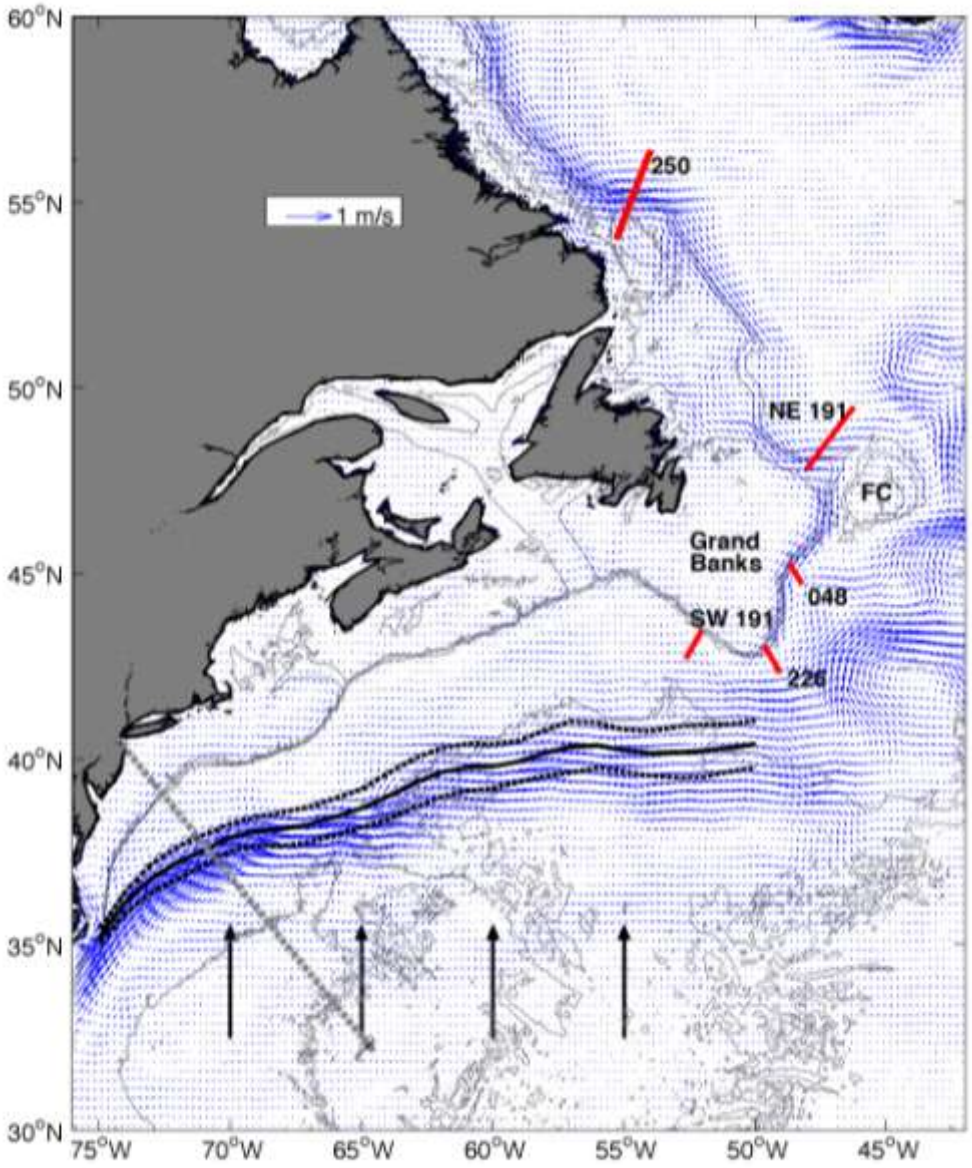

Figure 1. Mean geostrophic surface velocities showing the general large scale circulation and both the northeast-flowing Gulf Stream and southward-flowing Labrador Current (see text for explanation). Long-term mean position of the monthly-mean Gulf Stream North Wall (black solid line) and standard deviation (black dashed lines) are estimated from SST anomalies at every degree of longitude between 75° W and 50° W from the Canadian Marine Environmental Data Service. Also shown are the locations of: four longitude lines (black vertical arrows) on which annual mean positions of the Gulf Stream North Wall were measured, five outer-shelf altimeter along-track segments (red lines) for measuring upper-layer Labrador Current transport or sea height, the *M/V Oleander* transect (gray dashed line), the location of the Grand Banks, the Flemish Cap (FC), and the 500 m, 1000 m and 5000 m isobaths.

Changes in the latitudinal excursion of the GS path and their impact on its cross-stream sea-level gradient have also been linked to sea level rise along the Canadian and U.S. east coasts, a possible "slowing" of the GS, and increased frequency of coastal flooding (Boon, 2012; Ezer and Corlett, 2012; Sallenger *et al*., 2012; Ezer *et al*., 2013; Ezer and Atkinson, 2014). The extreme sea level rise noted using tide gauge data for a northeast region located between Cape Hatteras and Newfoundland may result from remote wind forcing (Andres *et al*., 2013) but also corresponded to the period of the 30% reduction in the AMOC from 2009-2010 (Goddard *et al*., 2015). Although both the GS and LC are driven by large-scale wind patterns over their respective gyres, with variability attributed to the North Atlantic Oscillation (NAO) (Taylor and Stephens, 1998; Marshall *et al*., 2001) studies suggest that thermohaline interactions between the GS, LC, DWBC, recirculation gyres, and shelf waters may also be important (Rossby, 1999; Rossby and Benway, 2000; Marshall *et al*., 2001, Chaudhuri *et al*., 2011). A significant part of this thermohaline interaction may result directly from the remaining equator-ward-flowing fraction of the surface LC and shelf waters releasing varying amounts of less-saline waters into the Slope Sea.

Evidence from low-frequency variations of sea surface salinity (SSS) shows large IAV (±1-2 PSU) that is coherent along the *M/V Oleander* line between New Jersey and Bermuda (Fig. 1) across both the continental shelf and slope water regions, supporting the hypothesis of a release of less-saline waters from the shelf into the Slope Sea (Rossby and Benway, 2000). Earlier work by Rossby (1999) suggests further that the well-noted annual shifting of the axis of the GS and its seasonal transport variations may result from annual variations of this "overflow" of freshwater from the north from an examination of seasonal and low frequency changes in dynamic height anomaly and transport of the GS (Sato and Rossby, 1995). Rossby (1999) speculates that such so-called "gyre interactions" may be operating on inter-annual time scales as well. Velocity observations at 52 m depth, just seaward of the shelf break along the *M/V Oleander* line, show a significant annual cycle of equator-ward transport with higher (lower) velocities during winter (summer) and are consistent with the GS displacement to the south by April (Rossby and Benway, 2000). IAV of the GS position shows similar behavior, with a southward displacement of the GS corresponding to time periods of higher equator-ward transport and lower SSS within both shelf and slope waters (Rossby and Benway, 2000). They suggested that since a larger volume flux along the shelf from the east into the Slope Sea must be accommodated without a significant thermocline depth increase, the GS must be displaced southward. In summary, these and other observations suggest the existence of an important upper-layer thermohaline mechanism that may partly determine the GS path over both annual and inter-annual time scales.

In work we present below, we examine long-term secular changes in the position of the GS "north wall" (GSNW) along with its IAV from 55° to 70° W longitude using satellite altimeter-derived data from 1993-2013 and compare our results with another published GSNW position index. We also examine long-term secular changes and IAV of upper layer LC transport and LC-related sea height variability at the shelf break in the western Labrador Sea and Grand Banks region for multi-year periods also using satellite altimeter data (following Han and Wang, 2006). Lastly, we compare the secular and inter-annual changes of LC transport with noted changes for the GSNW in both the time and frequency domains to test the thermohaline "overflow" hypothesis described above.

Data and Methods:

Merged satellite altimeter data were obtained from the Archiving Validation and Interpretation of Satellite Oceanographic (AVISO) data center (http://www.aviso.altimetry.fr) for the 21-year (1993-2013) period of record for this study. Mapped AVISO satellite altimeter data (daily, ¼° × ¼°) were used to compute the annual mean position of the GSNW using the 50-cm sea surface height anomaly contour measured along four longitude lines (Fig. 1) including 55°, 60°, 65°, and 70° W (Gangopadhyay *et al*., 2016). Gridded SSH data have been used here following Perez-Hernandez and Joyce (2014) and Gangopadhyay *et al*. (2016) to understand IAV of the GS path, because the latitudinal excursion of the GS between 75° and 55°W ranges between 100-300 km which is significantly larger than the error in averaging the fields from the ¼° resolution altimeter values. We compare our method to Taylor and Stephens (1998), who employed sea surface temperature (SST) oceanographic charts to detect the GSNW at six longitudes from 79° to 65° W and then computed a principal component Taylor-Stephens index (TSI) across all six longitudes for the 1966-2012 period. We note our current analysis extends farther to the east than Taylor and Stephens (1998) but not as far to the west. Other work by Joyce *et al*. (2000) used the location of the 15°C isotherm at 200-m depth to determine their GS path index from 75° to 50° W for the 1954-1989 period, thus bracketing our study longitudes. A recent study by Perez-Hernandez and Joyce (2014) used altimeter-derived monthly sea level anomalies determined along 16 points between 72° to 52° W to examine GS path changes.

Along-track AVISO satellite altimeter data were used to estimate annual mean LC transport across four outer-shelf altimeter track segments surrounding the Grand Banks (Fig. 1) after addition of model mean values computed using linear finite element solutions that excluded the Ekman surface current as described by Han and Wang (2006). The four segments cross the LC at nearly perpendicular angles (Han, 2006; Han *et al*., 2014): track 191NE in the southwestern Labrador Sea, track 048 along the southeastern Grand Banks, track 226 at the TGB, and track 191SW along the southwestern Grand Banks near 52° W (http://www.meds-sdmm.dfo-mpo.gc.ca/isdm-gdsi/azmp-pmza/climat/labrador/transport-eng.htm). The lengths of the altimeter sections were based upon the width of the mean LC at each location (Han, 2006). A fifth altimeter track segment, track 250, extends northeastward across Hamilton Bank (Figs. 1) and was used to compute a separate LC index upstream of the Grand Banks from sea height differences measured along-track between 54°N and 56.5°N. All along-track 250 passes were annually averaged for each year to compute the LC sea height index for the 1995-2010 time period. In summary, satellite altimeter data were used to examine the GSNW position, LC transport, and LC sea height changes for this study.

Spectral analyses of the relatively short, 21-year (1993-2013) GSNW and LC time series required use of an autoregressive (AR) modeling technique (Gangopadhyay *et al*., 2016). The AR spectral method has been shown to provide superior performance for short time series (Gangopadhyay *et al*., 1989). Each time series had the mean and trend subtracted, and normalized by their respective standard deviation prior to analysis using a sixth-order AR model; the order was chosen based on our experience of similar length time-series analyses (Gangopadhyay *et al*., 1989 (see Case study V, Fig. 5) ; Gangopadhyay *et al*., 2016). The confidence interval for spectral estimates by the AR methodology is based on approximate statistics (Kay, 1988) and remains constant across each spectrum because of the form of variance.

Results:

Gulf Stream North Wall (GSNW) Analysis

Each of the four GSNW annual mean position time series for the 1993-2013 period of record is shown along with its corresponding linear trend (Fig. 2). IAV of the GSNW position decreases westward from 55° to 70° W, along with the magnitude of the linear trend fitted to the data at each of the four longitudes that were analyzed (Table 1). A maximum linear southward secular trend of -0.10° y^{-1} or -11.08 km y^{-1} was measured at 55° W, decreasing westward to a small but insignificant trend at 70° W. While only the GSNW time series trend from 55°W (Fig. 2) displays a statistical significance of better than 95%, the significance at 60° and 65° W are just slightly lower at approximately 88%. Therefore, the tendency for both IAV and the magnitude of the computed (negative) trends to decrease rapidly in a westward direction is readily apparent. Thus, the computed secular trends signal a consistent southward movement of the GSNW between 55° and 65° W over the 21-year (1993-2013) period of record. We note again the lack of any trend of the GSNW at 70° W (Fig. 2), in agreement with Rossby *et al*., (2014) who found an insignificant long-term decrease in GS layer transport near 70° W along the *M/V Oleander* transect for a nearly identical 21-year period (1992-2012). However, additional analysis of the same data show weakening of the flux along the entire *M/V Oleander* transect in agreement with a weakening AMOC (Ezer, 2015). The co-variation of high (low) transport and northward (southward) position of the GS eastward of Cape Hatteras is supported by earlier modeling work by Chaudhuri *et al*. (2011).

Subtraction of the secular trend of GSNW movement for each of the time series located at 55°, 60°, 65°, and 70° W, results in time series of IAV of GSNW position residuals at each longitude. Comparisons between GSNW residuals (Fig. 3a, Table 1) show that the largest values consistently occur along eastern-most longitudes at 55° W (rms 1.13°) and at 60° W (rms 0.60°) with much-reduced values along western-most longitudes at 65° W (rms 0.31°) and 70° W (rms 0.24°). Furthermore, GSNW residuals at all four longitudes clearly show shorter period fluctuations and appear out-of-phase prior to 2003, with longer period fluctuations beginning during 2003 that appear largely in-phase across all four longitudes (Fig. 3a). Corresponding AR power spectra for GSNW residual time series at 55°, 60°, and 65° W clearly show both the shorter period (~2.5 year) and longer period (~5 year) fluctuation peaks (Fig. 3b) readily apparent in the time series. GSNW power spectra at 65° and 70° W show additional longer period peaks at ~10 years and ~7 years, respectively, with both an absence of the ~5 year peak and a shift of the shorter period peak to near ~3.5 years at 70° W (Fig. 3b).

Labrador Current (LC) Analysis

Annual mean along-stream LC transport time series for the 1993-2013 period of record measured across two outer-shelf altimeter track segments show highly significant decreasing linear trends of about -0.5 Sv per decade north of Flemish Pass (191NE) and along the eastern flank of the Grand Banks (048) (Fig. 4, Table 1). Further downstream, the trend of LC transport time series along track segment 226 near the TGB, while still decreasing (-0.2 Sv per decade), is not highly significant. However, the trend of LC transport time series for segment 191SW near 52° W along the southwestern flank of the Grand Banks increases at about +0.4 Sv per decade with somewhat higher significance (Fig. 4, Table 1).

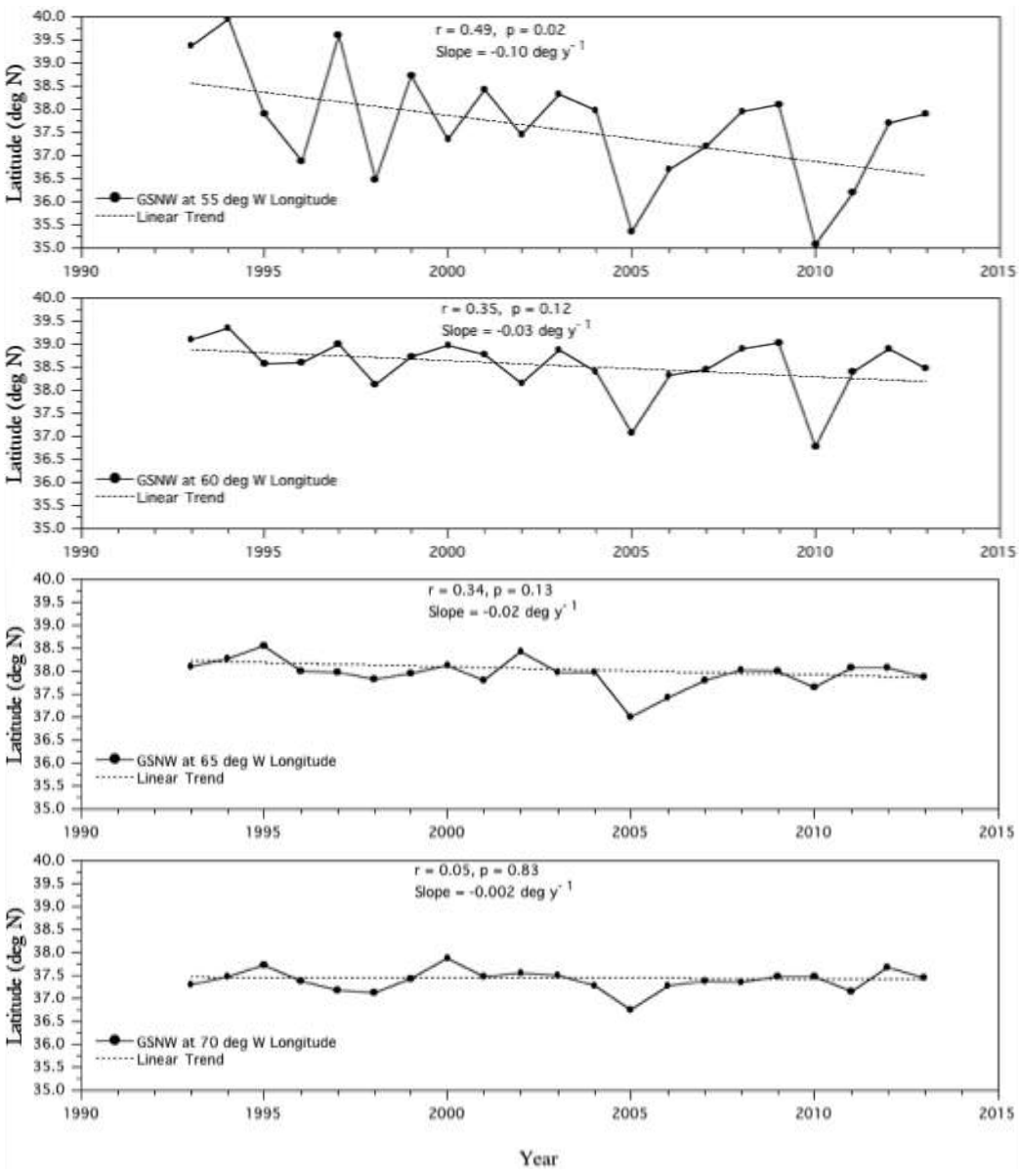

Figure 2. Annual mean latitude of the GSNW position computed along 55°, 60°, 65°, and 70° W from AVISO mapped altimeter data from 1993-2013, along with computed linear trends.

After removal of linear trends, IAV of LC transport residuals (Fig. 3a, Table 1) is large along downstream segments 226 near the TGB (rms 1.02 Sv), and 191SW near 52° W along the southwestern Grand Banks (rms 1.05 Sv). IAV is much reduced further upstream along segments 048 (rms 0.41 Sv) and 191NE (rms 0.29 Sv) along the eastern Grand Banks and north of Flemish Pass, respectively (Fig. 3a, Table 1). In addition, reduced-magnitude LC transport residuals along upstream segments 191NE and 048 appear to be in phase over most of the 21-year period of record, while the much larger residuals along downstream segments 226 and 191SW appear to be largely out-of-phase for the same period (Fig. 3a).

Table 1. Statistics of GSNW and LC Secular Trends and Inter-Annual Residuals

Significant correlation values ($p \leq 0.05$) are shown in bold.
N = 21 for all statistics shown.

GSNW Longitude	Y-intercept (° N), Slope (° Lat y^{-1}) Residual rms (° Lat)	r (p-value)
55° W	38.16, -0.10 1.13	**-0.49** **(0.02)**
60° W	38.87, -0.03 0.60	-0.35 (0.12)
65° W	38.22, -0.02 0.31	-0.34 (0.13)
70° W	37.45, 0.00 0.24	-0.05 (0.83)
LC Altimeter Segment	**Y-intercept (Sv), Slope (Sv y^{-1}) Residual rms (Sv)**	**r (p-value)**
191NE	6.55, -0.05 0.29	**-0.74** **(0.001)**
048	2.89, -0.05 0.41	**-0.65** **(0.001)**
226	1.80, -0.02 1.02	-0.10 (0.65)
191SW	0.64, 0.04 1.05	+0.22 (0.35)

Corresponding AR power spectra of LC transport residuals along upstream altimeter track segment 191NE, just north of Flemish pass, and downstream segments 226 at the TGB and 191SW near 52° W on the southwestern flank of the Grand Banks show both shorter period (~3 year) and longer period (~6-8 years) peaks (Fig. 3b). Upstream segment 048 located along the

eastern flank of the Grand Banks only shows the longer period peak (~8 years), with no evidence of the shorter period (~3 year) peak (Fig. 3b). Three of the eastern GSNW locations (65°W, 60°W and 55° W) peak at 5 years, while the southward flowing LC transport (across 191NE) shows a distinct 6-year peak (Fig. 3b). A number of GS and LC locations show peaks in the 2-to-3-year range. While these are individually significant, a coherence analysis could not be performed due to lack of degrees of freedom for the cross spectra for these short time-series. Note that these two periods (2-3 years, 5-6 years) also coincide with the characteristic periods for the atmospheric NAO forcing described by Gangopadhyay *et al*. (2016).

Discussion:

Combined Gulf Stream North Wall (GSNW) and Labrador Current (LC) Analysis

Inter-comparison of our GSNW position and LC transport time series allows the covariance of secular trends and IAV of the two western boundary currents to be examined in both the time and frequency domains. Subsequently, we also expand on a simplified test of the thermohaline "overflow" hypothesis described above using some basic assumptions and a simplified volume calculation methodology (Rossby, 1999; Rossby and Benway, 2000).

GSNW results from this study show a consistent long-term southward-directed secular trend for the GSNW at all four study longitudes that decreases westward from 55° to 70° W with a maximum (minimum) southward secular movement of approximately 220 km (4 km) at 55° W (70° W) for the 21-year (1993-2013) study period. However, although our results are in agreement with the southward shift reported by Ezer *et al*. (2013) between 70° and 74° W, they observed a northward shift between 68° and 70° W, showing that long-term shifts of the GS can be complex. Nevertheless, the large east-to-west difference in the secular movement of the GSNW over the two decades of this study suggests a mechanism that is maximal in the eastern portion of our study domain (near 55° W) such as southward LC transport. Other mechanisms, e.g., changes over the sub-tropical gyre may be important farther to the west (See Fig. 4 in Ezer, 2015). Interestingly, studies have shown that annual shifts of the GSNW are also maximal (~70 km) farthest east, near 63° W (secondary maximum of 30 km near 67° W) but are much smaller west of 70° W, using eight years of satellite-derived infrared SST imagery (Lee and Cornillon, 1995). In a recent study, Perez-Hernandez and Joyce (2014) show from monthly sea level anomalies that the leading mode of IAV of GS position are meridional shifts of approximately 100 km using their 16-point index, with higher modes representing GS meandering that vary with GS strength (Kelly *et al*., 2010). Their typical meridional shift of 100 km compares favorably with our mean RMS value of approximately 63 km computed as the average of the four RMS values shown in Table 1 after conversion to kilometers. Comparison of their highly-resolved monthly GS position time series with our annual mean GSNW position residuals shows some agreement, with extreme northward (southward) excursions during 1994-1995, 2000, 2006-2008, 2012 (1996, 1998, 2005, 2010). Similarly, GSNW path variability from this analysis at 65° and 70° W (Figs. 2 & 3a top panel) also shows agreement with the GS position determined along the *M/V Oleander* line as shown in Figure 3c by Ezer (2015). In addition, extreme southward GS excursions shown for 2005 and 2010 (Fig. 2 & 3a top panel) also coincide with extreme negative NAO states for those years, with 2010 corresponding to the period of weak AMOC noted in other studies (McCarthy *et al*., 2012; Ezer, 2015; Goddard *et al*., 2015)

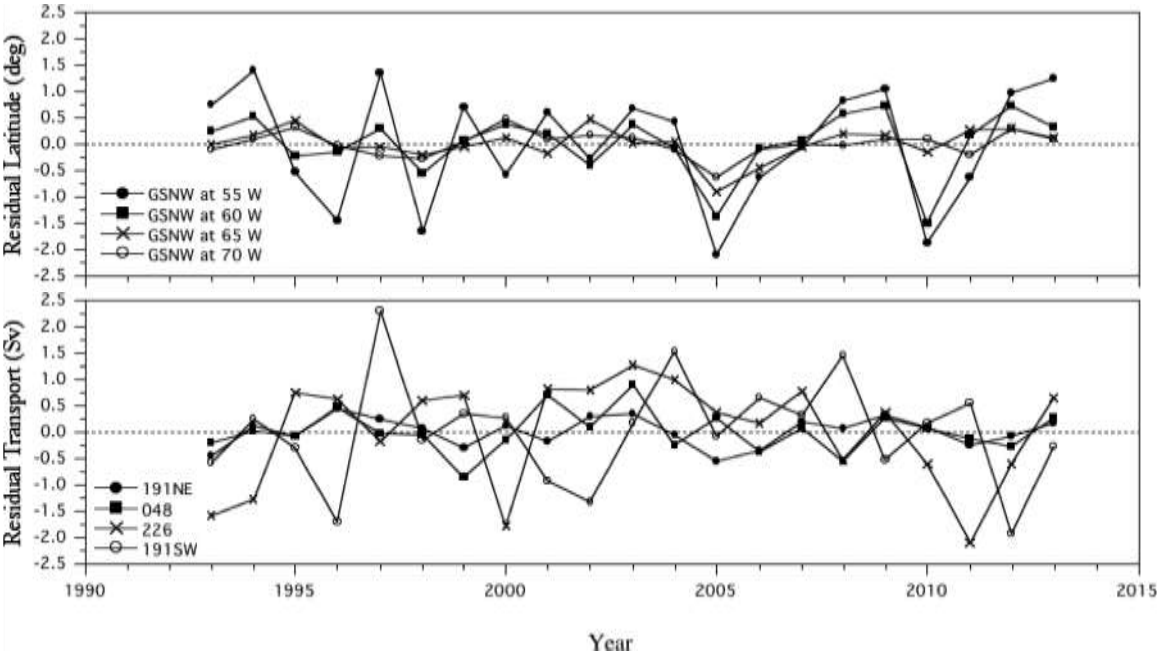

Figure 3a. (Top Panel) Annual mean GSNW position residuals along 55°, 60°, 65°, and 70° W from AVISO mapped altimeter data from 1993-2013, after subtraction of computed linear trends. (Bottom Panel) Annual mean Labrador Current transport residuals computed along outer-shelf altimeter track segments 191NE, 048, 226, and 191SW from AVISO along-track altimeter data from 1993-2013, after subtraction of linear trends.

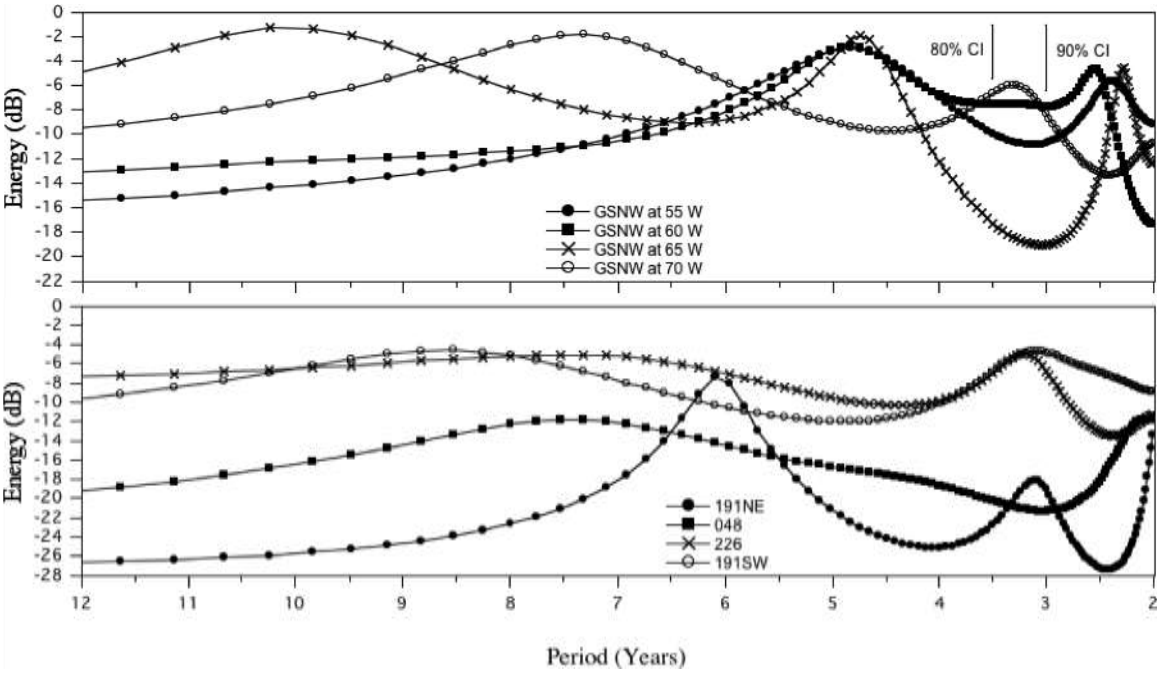

Figure 3b. (Top Panel) Normalized AR power spectra (order 6) of GSNW position residual time series from 55°, 60°, 65°, and 70° W in Fig. 3a above. (Bottom Panel) Normalized AR power spectra (order 6) of Labrador Current transport residual time series shown for altimeter track segments (191NE, 048, 226, and 191SW) in Fig. 3a above. Also shown are the 80% and 90% spectral confidence intervals (CI).

A recent study shows that during the last decade, SST in the Gulf of Maine (GOM) has increased at a rate faster than 99% of the global oceans (Pershing *et al*., 2015) and partially attributes this warming to a northward excursion of the GS, along with changes in both the Atlantic Multi-decadal Oscillation and Pacific Decadal Oscillation. Furthermore, they suggest that such changes may be partly responsible for the collapse of the cod fishery in New England waters, including the GOM. However, as shown in our analysis, the GSNW displays a clear southward trend over the past two decades at 55°, 60°, and 65° W, although displaying recent (2012-2013) large northward-directed residuals following the extreme southward GSNW position residuals for 2010 (Figs. 2 & 3a top panel). Specifically, while the long-term (21 years) southward trend at 70°W is not significant; it is significant at 85% or more at both 65° and 60°W. From 2005-2013 (period of study by Pershing *et al*. (2015)) our analysis does show a small northward trend in the GSNW at 70°W and 65°W, due largely to the extreme southward excursion of 2005, small northward shift during 2006-2009, southward movement for 2010 (65°W) or 2011 (70°W), followed by northward movement for 2012 (Fig. 2). In contrast, the eastern GS region at 60° and 55°W exhibits a clear periodicity of five years added to the significant long-term southward trend-line from 2005-2013 (Fig. 2). In any case, shelf SST north of Cape Hatteras, including the GOM, is warming at between 1.8-2.5 times faster than regional atmospheric trends and is thus similar to atmospheric trends over Labrador and the Arctic, supporting advection from the north (Shearman and Lentz, 2010), with noted sub-surface warming as well along the *M/V Oleander* expendable bathythermograph transect between 1977-2013 (Forsyth *et al*., 2015).

An examination of LC transport trends for the same 21-year (1993-2013) study period shows that they differ markedly from north-to-south along segments 191NE, 048, 226 and 191SW, with trends that transition from strongly negative in the north (191NE and 048) to positive in the south (191SW) on the southwestern flank of the Grand Banks in agreement with an analysis of data from some of the same altimeter sections (Han *et al*., 2014). Both our long-term secular analysis and the earlier trend analysis by Han *et al*., (2014) show that the LC transport off the northeastern Newfoundland slope is out-of-phase with that over the Scotian slope for nearly identical ~20-year periods of record. In addition, the increasing trend computed for segment 191SW near 52° W from our study (Fig. 4, Table 1) agrees with LC transport from segment 176 near 61° W off the central Scotian shelf (not shown) reported by Han *et al*., (2014). Furthermore, results from Han *et al*., (2014) also show that LC transport over the Newfoundland slope (Scotian slope) is positively (negatively) correlated with the winter North Atlantic Oscillation (NAO) index for inter-annual through decadal time scales, with the Grand Banks being a region of transition.

A shelf-wide near-surface salinity analysis (Bisagni, 2016) shows that large inter-annual anomalies are ubiquitous along the entire eastern seaboard of both the United States' and Canada's continental shelf, with strong variability located west of the TGB between 1973-2013. The same analysis shows near-surface salinity anomaly magnitudes increasing steadily from the Eastern Scotian Shelf to the DelMarVa/Hatteras shelf over a distance of ~1400 km and are synchronous (coherent at 0-year lag). These observations suggest that an along-shelf, wind-modulated, flux-variation model (Sundby and Drinkwater, 2007; Li *et al*., 2014), i.e., a varying flux across the mean along-shelf salinity gradient, as the most likely mechanism (Bisagni, 2016). In addition, *M/V Oleander* SSS data across the Middle Atlantic Bight region from New Jersey to Bermuda over a 21-year period (1978-1998) show synchronous salinity anomalies extending across both the shelf and Slope Sea regions (Rossby and Benway, 2000) also supporting large-

514

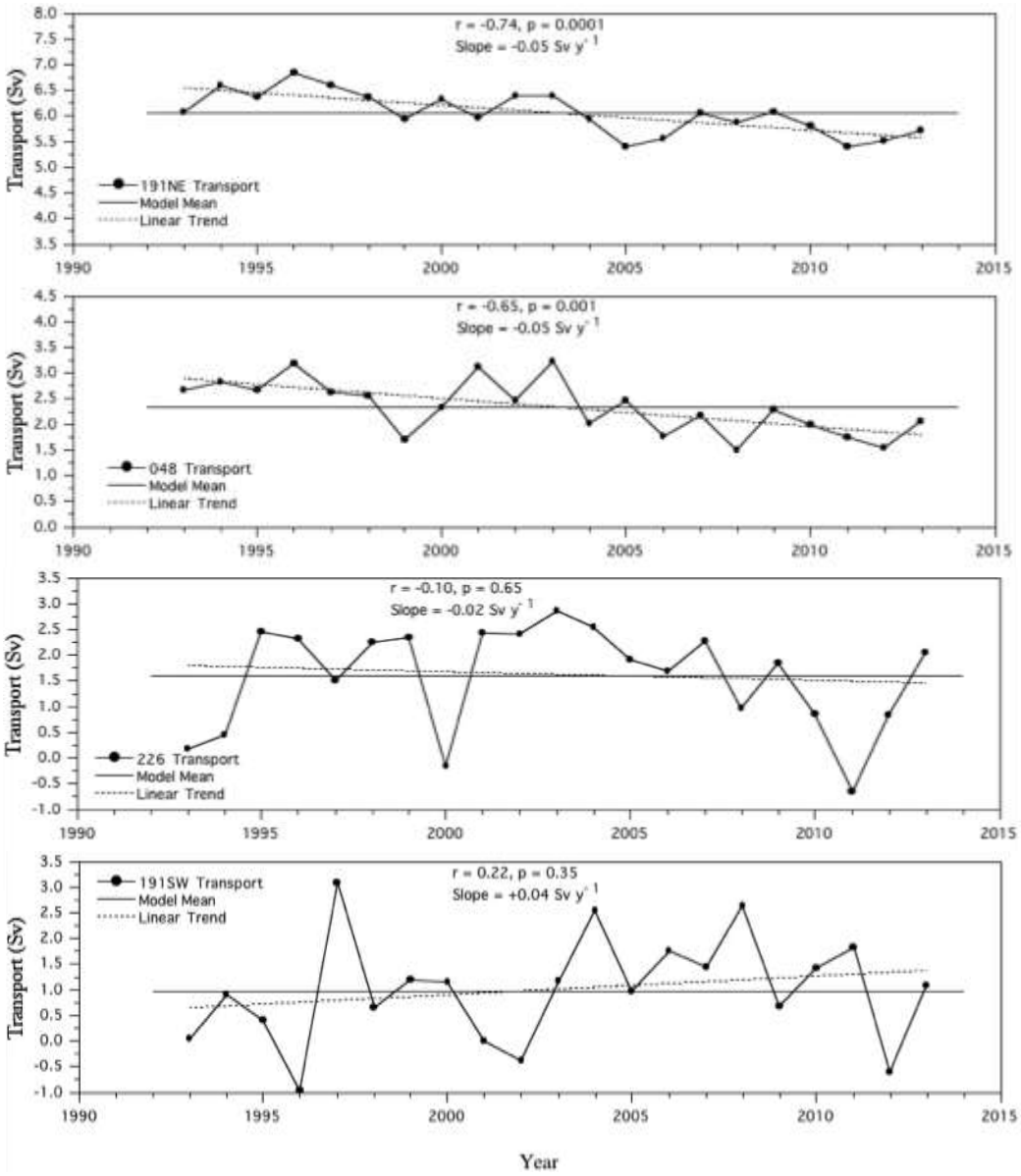
r = -0.74, p = 0.0001
Slope = -0.05 Sv y-1
191NE Transport
Model Mean
Linear Trend
Transport (Sv)
r = -0.65, p = 0.001
Slope = -0.05 Sv y-1
048 Transport
Model Mean
Linear Trend
Transport (Sv)
r = -0.10, p = 0.65
Slope = -0.02 Sv y-1
226 Transport
Model Mean
Linear Trend
Transport (Sv)
r = 0.22, p = 0.35
Slope = +0.04 Sv y-1
191SW Transport
Model Mean
Linear Trend
Transport (Sv)
Year

Figure 4. Annual mean Labrador Current transport computed across four outer-shelf altimeter track segments (191NE, 048, 226, and 191SW) shown in Figure 1 from AVISO along-track altimeter data from 1993-2013, along with the regression model mean across each segment, and computed linear trends. Positive (+) values signify equator-ward transport.

scale flux and temperature variations that may extend into the Slope Sea as discussed for slope water velocity anomalies (Peña-Molino and Joyce, 2008).

IAV of LC transport at the shelf break along segment 191SW near 52° W from this study is large (Fig. 4), with a strong negative (positive) transport anomaly corresponding to strong positive (negative) salinity anomalies as shown by other studies for 1996 and 1997, (Rossby and Benway, 2000; Flagg *et al*., 2006; Bisagni, 2016). Sea surface height along ground track segment 250 is chosen as representative of upstream LC transport within the Labrador Sea. This new upstream LC index is constructed along segment 250 between 54° and 56.5° N, using both ERS-2 and ENVISAT satellite missions, with the general structure of the SSH along this segment

being high to low SSH going in the offshore direction (towards higher latitudes), consistent with the Labrador Current flow at this location (Fig. 1). The LC index is computed from the height difference between 54° N and 56.5° N from each 250 pass and then annually averaged for the 1995 to 2010 time period.

Results from a comparison between annual TSI values with the more distal upstream segment 250 LC index within the Labrador Sea from 1995-2010 show the "broad scale" TSI of GS position to be highly correlated with the LC index (r=-0.68, significant at 95% level), with the LC index leading the TSI by 2 years (Fig. 5, top panel). More specifically, the LC index shows high values for 1996, 2001, 2006, and 2009 followed two years later by low TSI values; signifying that increases in our LC index along segment 250 are followed two years later by southward shifts in GS position. Similarly, lower values of our LC index observed for 1998, 2005, and 2008 are followed two years later by northward shifts in GS position (as represented by the TSI). The anomalously high LC index for 1996, high transport to the south, has been previously described as the strong LC 'pulse' in previous studies (e.g., Han, 2006). Farther to the south and near the TGB, comparison of the GSNW position residuals at 55° W with the downstream LC transport residuals along segment 191SW near 52° W at 0-year lag (not shown) does not show a significant relationship between the two signals ($r = 0.18$, $p = 0.43$). However, when the LC residual signal is lagged by +1 year (Fig. 5, lower panel), a significant negative correlation results ($r = -0.44$, $p = 0.05$), meaning that the previous year's LC transport residual near 52° W is related to the current year's GSNW position residual at 55° W, similar to the maximum 12 month (1-year) lag reported by Peña-Molino and Joyce (2008) for the relationship between cooler (warmer) slope water SST anomalies and more-southerly (northerly) shifts of the GS. A 1-year delay for the effect of changes in annual mean LC transport near 52° W on the GSNW position at 55° W does not seem unreasonable given the 2-year delay we find between the more-distal upstream segment 250 LC index and the broad scale TSI. This 1-year delay is in agreement with the 1-year delay reported earlier related to the Icelandic Low (Sanchez-Franks *et al*., 2016). Lastly, a significant correlation ($r = 0.48$, $p \leq 0.05$) was computed between the nearly contiguous *M/V Oleander*-derived southward-directed slope current (a LC extension) fluctuations and GS position values at 0-year lag for 1993-2012 (Ezer, 2015), and supports our correlation results near 52° W after consideration of the sign conventions used for each analysis.

A recent study by Gangopadhyay *et al*., (2016) has shown that the GS has behaved differently along its path from 75° W to 55° W over the last four decades. Specifically, the GSNW latitudinal excursion variability west of 60° W, exhibits a dominant time scale of 8-10 years, while eastward from 65° W, a 4-5 year time scale was also present, with a 2.5-3.5 year time scale being present at all four longitudes from this study (Figs. 3a and 3b). The 8-10 year time scale present from 70° W to 65° W is clearly related to the NAO signal as shown by other investigators (Cook *et al*., 1998; Wunsch, 1999) and also GS intensity and coastal sea level (Ezer *et al*., 2013). We can also speculate further that both the 4-5 year and the 2.5-3.5 year IAV may also be related to the NAO due to possible interactions between the NAO and the LC as described by Han *et al*. (2014), caused by variations in the strength and location of the Icelandic Low for a lag of +1 year (Sanchez-Franks *et al*., 2016). The co-plot of the GSNW residual time series at 55° W with the LC residual time series along segment 191SW near 52° W does show a significant relationship between the two signals when the LC residual signal is lagged by +1 year, i.e., changes in the LC transport near 52° W lead the GSNW position changes by one year (Fig. 5, lower panel).

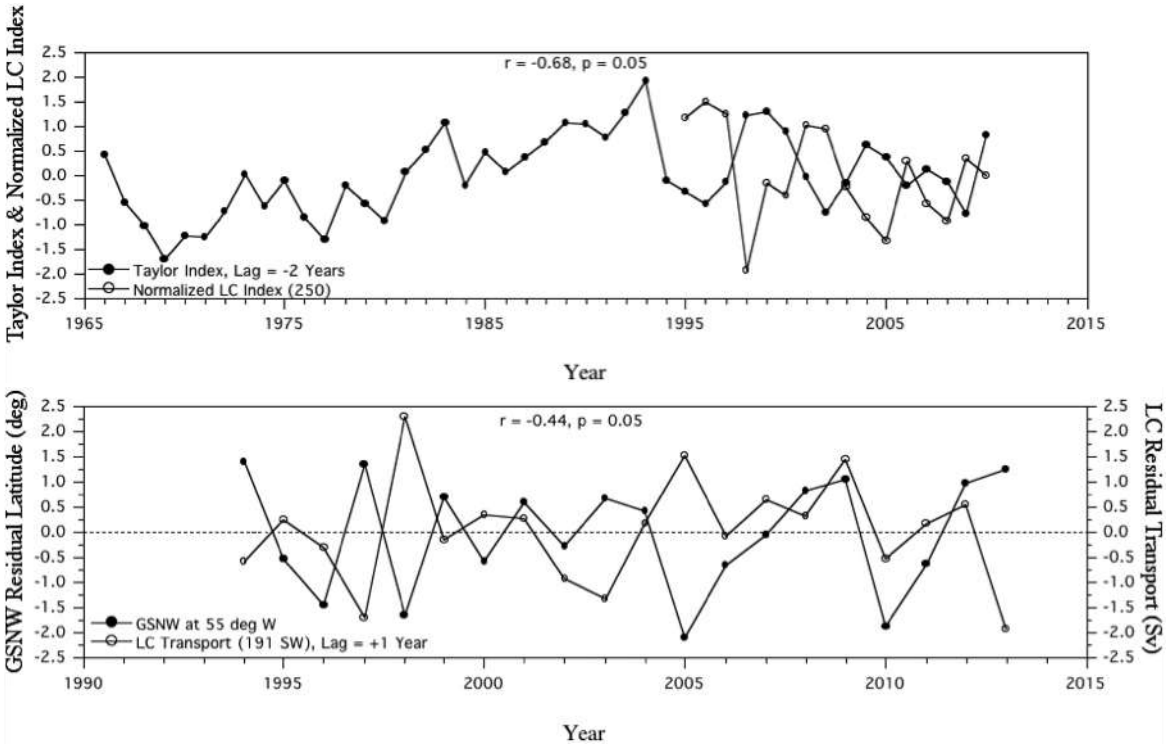

Figure 5 (Top Panel) Annual mean TSI (-2-year lag) along with annual mean LC index for pass 250 in the Labrador Sea from Fig. 1. Correlation coefficient and p-value (n = 16) for TSI at -2-year lag. Note that the -2-year lag applied to the TSI as shown above is equivalent to a +2-year lag applied to the LC index as described in the text. (Bottom Panel) Annual mean GSNW position residuals along 55° W along with annual mean LC transport residuals (+1-year lag) computed along segment 191SW near 52° W. Correlation coefficient and p-value (n = 20) for LC at +1-year lag.

A Possible Model

A volume flux calculation by Rossby (1999) was used to estimate the annual movement of the GSNW along the southern boundary of the Slope Sea due to a hypothesized annual baroclinic transport cycle of 0.5 Sv across the shelf-slope front, i.e., a "spilling" of less-saline waters into the Slope Sea from the shelf. Assuming no change in the depth of the Slope Sea upper layer (200 m), the volume flux calculation resulted in an annual GS movement of 42 km, a number that is midway between the two maximum annual values reported using satellite-derived SST data by Lee and Cornillon (1995). Alternatively, the annual baroclinic transport could also have been accommodated by an increase in Slope Sea upper layer depth of 29 m. Rossby (1999) further describes how both the annual cycle in the position of the GS, i.e., north during fall and south during spring (Iselin, 1940; Watts, 1983) and the 8 Sv annual cycle in GS transport (maximal during early summer as reported by Sato and Rossby (1995)) may be related to the June timing of the maximum difference in the Fofonoff potential energy anomaly (PEA) values. Rossby's hypothesis is based upon changes in layer depth across the GS measured from the Slope Sea to the Sargasso Sea resulting in the annual GS cycles described above (Sato and Rossby, 1995).

We extended the volume flux calculation methodology described by Rossby (1999), assuming a simplified length and depth (2000 km × 200 m) for the Slope Sea located north of the

GS. Integrating the calculated positive long-term trend of LC transport into the Slope Sea at 52° W (segment 191SW) over the 1993-2013 period (Table 1), we can account for 68.4% (0.53° latitude) of the mean southward-directed secular shift of the GSNW (0.77° latitude) averaged across all four GSNW longitudes used herein. A second volume flux calculation using the measured inter-annual LC rms residual of +1.04 Sv at 52° W integrated over one year results in a corresponding southward residual for the GSNW of 79 km, or 63% of the observed 125.6 km (1.13°) GSNW rms residual at 55° W. We speculate that the remaining 37% of the unexplained GSNW rms residual may result from IAV of shelf water volume (Mountain, 2003) and position of the shelf-slope front separating shelf and slope waters (Bisagni *et al*., 2009).

In summary, our secular and inter-annual volume flux calculations using measured LC transport numbers, although crude, result in plausible secular and inter-annual GSNW fluctuation magnitudes. This level of agreement supports direct interaction between the upper layers of the sub-polar and sub-tropical gyres within the North Atlantic over secular and inter-annual time scales as suggested by Rossby (1999) and Rossby and Benway (2000). However, the proposed simple volume flux mechanism, although plausible, should be compared with future long-term analyses of computed Fofonoff PEA values in both the Slope Sea and Sargasso Sea as computed by Sato and Rossby (1995) in their dynamical analysis. While the secular and inter-annual time scales of GSNW variability are most likely due to NAO modulation of the North Atlantic circulation including LC transport as suggested by Marshall *et al*., (2001), this study shows that additional research is needed to confirm the actual dynamical mechanism related to gyre interactions. Important needs are much longer records of GSNW positions and LC transports to determine if the southward secular trend of the GSNW observed from 1993-2013 will continue and if these changes are related to variations in LC transport from the north.

Summary and Conclusions:

Recent work has shown that changes in the GS position after its separation from the coast at Cape Hatteras may be a key to the understanding of changes in the AMOC, sea level variability and coastal flooding along the eastern seaboard of North America, and recently observed changes in coastal and offshore ecosystems. In this study we compared secular change and IAV of the GSNW position between 55° and 70° W with equator-ward LC transport along the southwestern Grand Banks near 52° W and a LC index in the western Labrador Sea using approximately two decades of satellite altimeter data.

1) Results at 55°, 60°, and 65° W show a significant southward (negative) secular trend for the GSNW, decreasing to a small but insignificant southward trend at 70° W, with IAV of de-trended GSNW position residuals also decreasing to the west, but largely in phase, especially from 2003-2013.
2) The long-term secular trend of annual mean upper layer (200 m) LC transport near 52° W is positive with a transition to negative trends near the Tail of the Grand Banks (TGB) and into the Labrador Sea along the eastern Grand Banks in agreement with previous work.
3) Secular changes we report for the GSNW and LC have occurred during the time of a weakening AMOC over the past decade and that both past and ongoing AMOC monitoring efforts (RAPID and OSNAP) will continue to provide a more complete picture of the total AMOC over time.
4) IAV of the Taylor-Stephens Index (TSI) computed from the first principal component of the GSNW position measured from 79° to 65° W shows a significant relationship with IAV of our LC Index computed along altimeter ground track 250 located across Hamilton Bank (north of the Grand Banks) in the western Labrador Sea from 1995-2010. Increased (decreased) sea height differences along altimeter ground track 250 are significantly correlated ($r = -0.68$, $p = 0.05$) with a more southward (northward) TSI two years later (a LC index lag of +2-years).
5) IAV of LC transport residuals near 52° W along the southwestern Grand Banks are significantly correlated at a lag of +1-year ($r = -0.44$, $p = 0.05$) with IAV of GSNW position residuals at 55° W, with positive (negative) LC transport residuals corresponding to southward (northward) GSNW positions, i.e., changes in the LC transport lead the GSNW position changes by one year.
6) Spectral analysis of IAV reveals corresponding spectral peaks at 5-7 years and 2-3 years for the North Atlantic Oscillation (NAO), GSNW (70°-55°W) and LC transport near 52° W for the 1993-2013 period suggesting a connection between these phenomena.
7) An upper-layer (200 m) slope water volume calculation using the LC IAV rms residual of +1.04 Sv near 52° W results in an estimated GSNW IAV position residual of 79 km, or 63% of the observed 125.6 km (1.13°) rms value at 55° W.
8) A similar upper-layer slope water volume calculation using the positive long-term, upper-layer LC transport trend accounts for 68% of the mean observed secular southward shift of the GSNW between 55° and 70°W over the 1993-2013 period.
9) Our work provides additional observational evidence supporting interactions between the upper layers of the sub-polar and sub-tropical gyres within the North Atlantic over both secular and inter-annual time scales as suggested in previous studies. This interaction may be in addition to and a direct result of wind-forcing supplied by changes in the NAO over the entire North Atlantic Ocean as described by others (Marshall *et al*., 2001; Chaudhuri *et al*., 2011).

Acknowledgements:

This work was supported in part through a recent sabbatical (Bisagni) from the University of Massachusetts, Dartmouth, hosted by G. Gawarkiewicz at the Woods Hole Oceanographic Institution (WHOI), Woods Hole, Massachusetts. This work was also partly supported (Gangopadhyay) by NSF Grants OCE-0815679 and OCE-0535379, and NOAA Grant NA11NOS0120038 [for the implementation of the Mid-Atlantic Regional Association Coastal Ocean Observing System (MARACOOS)] during the development of some of the analyses presented herein. This work was also partly supported (Sanchez-Franks) by NSF Grant OCE-0825418. We are grateful to Dr. A. Schmidt, University of Massachusetts, Dartmouth, for providing the Gulf Stream North Wall position data, to Dr. G. Han, Northwest Atlantic Fisheries Centre, Fisheries and Oceans Canada, St. John's, Newfoundland, for providing the Labrador Current transport data, and to five anonymous reviewers for their thoughtful comments and suggestions. AS-F thanks C. N. Flagg, H. T. Rossby and K. A. Donohue for feedback and comments on the Labrador Current and Gulf Stream interaction part of the analysis.

752 **References:**
753

754 Andres, M., Gawarkiewicz, G. G. & Toole, J. M. Interannual sea level variability in the western
755 North Atlantic: Regional forcing and remote response. *Geophys. Res. Lett*., **40**, 5915-5919,
756 doi: 10.1002/2013GL058013 (2013)

757 Bisagni, J. J., Kim, H-S., & Chaudhuri, A. Inter-annual variability of the shelf slope front
758 position between 75° and 50° W. *J. Mar. Syst.,* doi:10.1016/j.jmarsys.2008.11.020 (2009)

759 Bisagni, J. J. Salinity variability along the eastern continental shelf of Canada and the United
760 States, 1973-2013. *Cont. Shelf Res*. **126**, 89-109 (2016)

761 Boon, J. D. Evidence of sea level acceleration at U.S. and Canadian tide stations, Atlantic Coast,
762 North America. *J. Coastal Res*. **28**, 1437-1445 (2012)

763 Chaudhuri, A. H., Gangopadhyay, A., & Bisagni, J. J. Response of the western North Atlantic
764 basin to characteristic high and low phases of the North Atlantic Oscillation. *Ocean*
765 *Modell.* **39**, 220-232 (2011)

766 Cook, E. R., D'Arrigo, R. D., & Briffa, K. R. The North Atlantic Oscillation and its expression
767 in circum-Atlantic tree-ring chronologies from North America and Europe. *Holocene*, **8**, 9-
768 17 (1998)

769 Ezer, T. & Corlett, W. B. Is sea level rise accelerating in the Chesapeake Bay? A demonstration
770 of a novel new approach for analyzing sea level data. *Geophys. Res. Lett*. **39**, L19605
771 (2012)

772 Ezer, T., Atkinson, L. P., Corlett, W. B. & Blanco, J. L. Gulf Stream's induced sea level rise and
773 variability along the U.S. mid-Atlantic coast. *J. Geophys. Res.* **118**, 685-697 (2013)

774 Ezer T. & Atkinson L. P., Accelerated flooding along the U.S. East Coast: On the impact of sea-
775 level rise, tides, storms, the Gulf Stream, and the North Atlantic Oscillations. *Earth's*
776 *Future* **2(8)**:362-382. doi: 10.1002/2014EF000252, (2014)
777
778 Ezer, T., Detecting changes in the transport of the Gulf Stream and the Atlantic overturning
779 circulation from coastal sea level data: The extreme decline in 2009-2010 and estimated
780 variations for 1935-2012, *Glob. Planet. Change*, **129**, 23-36,
781 doi:10.1016/j.gloplacha.2015.03.002, (2015).
782
783 Flagg, C. N, Dunn, M., Wang, D-P, Rossby, H. T., & Benway, R. L. A study of the currents of
784 the outer shelf and upper slope from a decade of shipboard ADCP observations in the
785 Middle Atlantic Bight. *J. Geophys. Res.* **111** , C06003, doi:10.1029/2005JC003116 (2006)

786 Forsyth, J. S. T., Andres, M. & Gawarkiewicz, G. G. Recent accelerated warming of the
787 continental shelf off New Jersey: Observations from the *CMV Oleander* expendable
788 bathythermograph line. *J. Geophys. Res.* **120** , doi:10.1002/2014JC010516 (2015)

789 Gangopadhyay, A., Cornillon, P. & Jackson, L. B. Autoregressive modeling for spectral analysis
790 of oceanographic data. *J. Geophys. Res.* **94** , 16215–16226 (1989)

791 Gangopadhyay, A., Chaudhuri, A. H., & Taylor. A. H. On the nature of temporal variability of
792 the Gulf Stream Path from 75° to 55°W. *Earth Interact*. **20,** (9) 17 pp. (2016)

793 Goddard P. B., Yin J., Griffies S. M., Zhang S., An extreme event of sea-level rise along the
794 Northeast coast of North America in 2009–2010. *Nature Comm.* **6**
795 doi:10.1038/ncomms7346 (2015)
796
797 Han, G. Low-frequency variability of sea level and currents off Newfoundland. *Adv. Space Res.*
798 **38,** 2141-2161 (2006)
799
800 Han G. & Wang Z. Monthly-mean circulation in the Flemish Cap region: a modeling study,
801 *Estuar. Coastal Model.,* ASCE, 138-154, (2006)
802
803 Han, G., Chen, N. & Ma, Z. Is there a north-south phase shift in the surface Labrador Current
804 transport on the interannual-to-decadal scale? *J. Geophys. Res.* **119**, 276-287 (2014)

805 Iselin, C. O. D. Preliminary report on long period variations in the transport of the Gulf Stream
806 system. *Pap. Phys. Oceanogr. and Meteor*. **8**(1), 40 (1940)

807 Joyce, T. M., Deser, C., & Spall, M. A. The relation between decadal variability of subtropical
808 mode water and the North Atlantic Oscillation. *J. Clim*. **13**, 2550-2569 (2000)

809 Joyce, T. M., Zhang, R. On the path of the Gulf Stream and the Atlantic meridional overturning
810 circulation. *J. Clim.*, **23,** 3146-3154, doi:10.1175/2010JCLI3310.1 (2010)
811
812 Kay, S. M. *Modern spectral estimation: theory and application*. Prentice-Hall, Englewood
813 Cliffs, NJ USA (1988)

814 Kelly, K. A., Small, R. J., Samelson, R. M., Qiu B., Joyce, T. M., Kwon, Y-O., & Cronin, M. F.
815 Western boundary currents and frontal air-sea interaction: Gulf Stream and Kuroshio
816 Extension. *J. Clim.*, **23,** 5644-5667, doi:10.1175/2010JCLI3346.1 (2010)

817 Lee, T. & Cornillon, P. Temporal variation of meandering intensity and domain-wide lateral
818 oscillations of the Gulf Stream. *J. Geophys. Res.* **100** , 13603–13613 (1995)

819 Li, Y., Ji, R., Fratantoni, P. S., Chen, C. , Hare, J. A., Davis, C. S. & Beardsley, R. C. Wind-
820 induced inter-annual variability of sea level slope, alongshelf flow, and surface salinity on
821 the Northwest Atlantic shelf, *J. Geophys. Res*. **119**, 2462–2479 (2014)

822 Marshall, J., Johnson, H., & Goodman, J. A study of the interaction of the North Atlantic
823 oscillation and ocean circulation. *J. Clim.,* **14,** 1399-1421 (2001)

824

825 McCarthy, G., Frajka-Williams, E., Johns, W. E., Baringer, M. O., Meinen, C. S., Bryden, H. L.,
826 Rayner, D., Duchez, A., Roberts, C., & Cunningham, S. A. Observed inter-annual
827 variability of the Atlantic meridional overturning circulation at 26.5°N. *Geophys. Res.*
828 *Lett*., **39**, L19609, doi: 10.1029/2012GL052933 (2012)

829 Mountain, D. G. Variability in the properties of Shelf Water in the Middle Atlantic Bight, 1977-
830 1999. *J. Geophys. Res*. **108**, doi:10.1029/2001JC001044 (2003)

831 Peña-Molino, B. and Joyce, T. M. Variability in the Slope Water and its relation to the Gulf
832 Stream path. *Geophys. Res. Lett*. **35**, doi:10.1029/2007GL032183 (2008)

833 Perez-Hernandez, M. D., & Joyce, T. M. Two modes of Gulf Stream variability revealed in the
834 last two decades of satellite altimeter data. *J. Phys. Oceanogr.* **44**, 149-163 (2014)

835 Pershing, A. J., Alexander, M. A., Hernandez, C. M., Kerr, L. A., Le Bris, A., Mills, K. E., Nye,
836 J. A., Record, N. R., Scannell, H. A., Scott, J. D., Sherwood, G. D., Thomas, A. C. Slow
837 adaptation in the face of rapid warming leads to collapse of the Gulf of Maine cod fishery.
838 *Science* **350**, 809-812 (2015)

839 Rossby, T. On gyre interactions. *Deep-Sea Res. II* **46**, 139-164 (1999)

840 Rossby, T. & Benway, R. L. Slow variations in mean path of the Gulf Stream east of Cape
841 Hatteras. *Geophys. Res. Lett.* **27**, 117-120 (2000)

842 Rossby, T., Flagg, C. N., Donohue, K., Sanchez-Franks, A. & Lillibridge, J. On the long-term
843 stability of Gulf Stream transport based on 20 years of direct measurements. *Geophys. Res.*
844 *Lett.* **41**, 114-120 (2014)

845 Sallenger, A. H., Doran, K. S. & Howd, P. A. Hotspot of accelerated sea level rise on the
846 Atlantic coast of North America. *Nature Clim. Ch.* **2**, 884-888 (2012)

847 Sanchez-Franks, A., & Zhang R. Impact of the Atlantic Meridional Overturning Circulation on
848 the decadal variability of the Gulf Stream path and regional chlorophyll and nutrient
849 concentrations, *Geophys. Res. Lett.*, 42, 9889–9887 (2015), doi:10.1002/2015GL066262.

850 Sanchez-Franks, A., Hameed, S., & Wilson, R. E. The Icelandic low as a predictor of the Gulf
851 Stream north wall position. *J. Phys. Oceanogr.* **46**, 817-826 (2016)

852 Sato, O. T. & Rossby, T. Seasonal and low frequency variations in dynamic height and transport
853 of the Gulf Stream. *Deep-Sea Res.* **42**, 149-164 (1995)

854 Shearman, R. K. & Lentz, S. J. Long-term sea surface temperature variability along the U.S. east
855 coast. *J. Phys. Oceanogr.* **40**, 1004-1017 (2010)

856

857 Smeed, D. A., McCarthy, G. D., Cunningham, S. A., Frajka-Williams, E., Rayner, D., Johns,
858 W. E., Meinen, C. S., Baringer, M. O., Moat, B. I., Duchez, A., & Bryden, H. L.
859 Observed decline of the Atlantic meridional overturning circulation 2004-2012. *Ocean*
860 *Sci*. **10**, 29-38 (2014)
861
862 Sundby, S. & Drinkwater, K. On the mechanisms behind salinity anomaly signals of the northern
863 North Atlantic. *Prog. In Oceanogr*. **73**: 190-202 (2007)

864 Taylor, A. H. & Stephens, J. A. The North Atlantic Oscillation and the latitude of the Gulf
865 Stream. *Tellus* **50A**: 134-142 (1998)

866 Toole, J. M., Curry, R. G., Joyce, T. M., McCartney, M. & Peña-Molino, B. Transport of the
867 North Atlantic deep western boundary current about 39°N, 70°W: 2004-2008. *Deep-Sea*
868 *Res. II* **58**, 1768-1780 (2011)

869 Watts, D. R. Gulf Stream variability. *Eddies in Marine Science*, A. R. Robinson, Ed., Springer-
870 Verlag 114-167 (1983)

871 Wunsch, C. The interpretation of short climate records, with comments on the North Atlantic and
872 Southern Oscillation. *Bull. Amer. Meteor. Soc*. **80**, 245-255 (1999)

873 Yashayaev, I., Seidov, D. & Demirov, E. A new collective view of oceanography of the Arctic
874 and North Atlantic basins. *Prog. In Oceanogr*. **132**: 1-21 (2015)